Journal of Membrane Science & Research

journal homepage: www.msrjournal.com

Research Paper

Comparative Study of Separation Performance of Hydroxy Sodalite Infused Polysulfone (HSOD/PSf) and Silica Sodalite Infused Polysulfone (SSOD/PSf) Membrane for Acid Mine Drainage Treatment

Nobuhle C. Ntshangase [1], Olawumi O. Sadare [2], Michael O. Daramola [2,*]

[1] *School of Chemical and Metallurgical Engineering, Faculty of Engineering and Built Environment, University of the Witwatersrand, Johannesburg, Private Bag 3, Wits 2050, South Africa*
[2] *Department of Chemical Engineering, Faculty of Engineering, Built Environment and Information Technology, University of Pretoria, Hatfield 0028, Pretoria, South Africa*

Article info

Received 2021-12-07
Revised 2022-01-19
Accepted 2022-02-04
Available online 2022-02-04

Keywords

Acid mine drainage
Hydroxy sodalite
Heavy metals
Silica sodalite
Membranes
Topotactic conversion

Highlights

- Silica sodalite crystals prepared via topotactic conversion
- Physicochemical characterisation of the crystals carried out
- Used in prepared sodalite-infused PSf membrane and tested for the first time for AMD treatment.
- The developed membranes outperformed the pure PSf membrane tested under similar conditions.

Graphical abstract

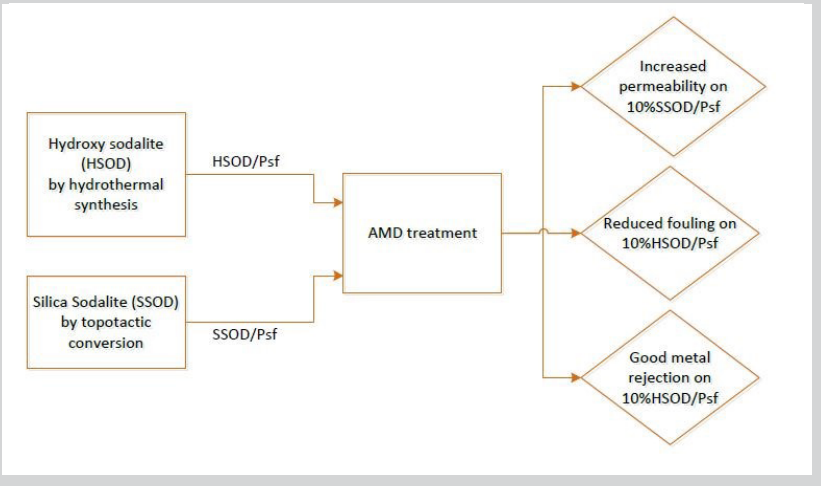

Abstract

Silica Sodalite (SSOD) was synthesized by topotactic conversion and hydroxy sodalite (HSOD) by hydrothermal synthesis in this study for comparison in membrane performance during acid mine drainage (AMD) treatment. Consequently, two membranes, SSOD/PSf and HSOD/PSf membranes at different nanoparticles loading (5wt. % and 10wt. %) were prepared. The morphology, textural property, crystallinity, surface chemistry, and thermal stability of the synthesized nanoparticles were checked using Scanning Electron Microscopy (SEM), N_2 physisorption at 77 K, X-Ray Diffraction (XRD), Fourier Transform Infra-red (FTIR), and Thermogravimetry analyser (TGA), respectively. The hydrophilicity and the mechanical strength of the as-prepared membranes were obtained using contact angle measurement and a nano-tensile analyser, respectively. The RUB-15 conversion to SSOD was confirmed with the preserved sheet-like shape of the nanoparticles, and the absence of CH_3 deformation vibrations at 1488 cm^{-1}. The absence of the –OH bond in the 2900-3600 cm^{-1} region of the FTIR spectra further confirmed the formation of SSOD. The SEM images showed a successful infusion of nanoparticles. Loading the membranes with SSOD enhanced the membrane permeability from 0.02 $g.h^{-1}.cm^{-2}$ for PSf to 0.21 $g.h^{-1}.cm^{-2}$ for 10%SSOD/PSf at 5 bar. The 10%HSOD/PSf membrane had good metal ion rejection with 75 %, 66 %, 61 %, 57 %, 52 %, and 38 % for Mg^{2+}, Fe^{3+}, Mn^{2+}, Ca^{2+}, Al^{3+} and Na^{2+}, respectively, while Al^{3+} had the highest rejection (89%) in the 10%SSOD/PSf membrane. This study provides a platform for further study on the improvement of SSOD usage in AMD treatment as it shows enhanced permeability with promising rejection.

1. Introduction

South Africa is one of the countries that depend on mining and agriculture for its economic development. These sectors are much dependent on water, and the mining sector reduces the productivity of the agricultural land due to pollution by acid mine drainage (AMD) [1]. AMD is identified as having a low

* Corresponding author: michael.daramola@up.aac.za (M.O. Daramola)

DOI: 10.22079/JMSR.2022.544024.1516

pH, high concentration of sulphates, and high concentration of heavy metals and metalloids [2]. It is formed in both gold and coal mines when sulphide-bearing minerals are exposed to oxidizing bacteria, water, and oxygen [3]. Generally, there is no standard method to treat AMD as the contents of this wastewater largely depends on its source. The rate of AMD formation is known to be influenced by five factors, namely, sulphides morphology, oxygen concentration, wetting and drying cycles, bacteria and acid consuming material, and the geological history of the sulphides [4].

Conventional treatment methods used to treat AMD are classified as passive or active methods. Passive methods are more effective in abandoned mines as they have the potential for low operational cost and maintenance [5]. While active treatment systems have higher limits of acidity (<10 000 mg $CaCO_3$/L) and acidity loads (<50 000 kg $CaCO_3$/day), their application is limited by their economic viability [4]. The interest of researchers has been drawn toward membrane applications for the treatment of AMD. This is because of their efficiency, selectivity, reliability, and adaptation to changes in flow volume [6]. Researchers have investigated the effectiveness of membrane technology for the removal of heavy metals from contaminated wastewater [6-8].

In the context of membranes in treating heavy metals contaminated water, thermally driven membranes like membrane distillation have been investigated for the treatment of AMD [9]. Although recommended because of very high metal rejections, membrane distillation technology is limited by the increased rate of fouling resulting in a reduction of flux and the costs associated with thermal energy consumption [10]. Reverse osmosis is one of the favoured membrane systems in the treatment of AMD [11]. However, the challenge with reverse osmosis is that it is not effective when the feed is too concentrated in heavy metals, hence, often requires a pre-treatment step. Reverse osmosis also produces a brine stream which is expensive to dispose [11]. Pressure-driven conventional membranes like microfiltration [12], nanofiltration [13], and ultrafiltration [14] with less energy demand, when compared to reverse osmosis have been investigated. However, these membranes are often coupled with other technologies to improve their performance. Focus has shifted to mixed matrix membranes (MMMs) to treat AMD. Mixed matrix membranes (MMMs) are modified conventional membranes which incorporate nanoparticles as filler materials [8]. The filler material infused into a polymer has a great influence on the MMM performance. Fillers like chitosan [8,15,16] and HSOD [6] have been reported for the removal of heavy metals from wastewater.

This study focused on the use of HSOD nanoparticles as a filler material. This is because HSOD has shown the potential to treat a variety of wastewater including separation, water/Pb^{2+} [17], water/alcohol [18], seawater [19], and acid mine drainage [6]. The removal of heavy metals using HSOD infused polyethersulfone (PES) membrane was investigated by Daramola et al. [6]. They obtained rejections of 57.5% (Pb^{2+}), 50% (Mg^{2+}), 30% (Al^{3+}), 17.6% (Cu^{2+}), and 6% (Mn^{2+}). The use of HSOD/PES membrane showed potential in removing heavy metals. The limited performance was attributed to the ineffective usage of the HSOD micropores because guest species (water) which was acquired during hydrothermal synthesis were trapped in the cages. Moteki, et al. [20] however indicated that if the guest species is to be removed at temperatures above 400°C by dehydration, the framework structure would collapse. Silica sodalite (SSOD), a type of zeolite synthesized by topotactic conversion has a high porosity as it does not have occluded matter [21]. To the best of our knowledge, there is no reported investigation on the treatment of AMD wastewater using this SSOD. SSOD will be investigated for heavy metals removal and compared to an HSOD-infused PSf membrane in this study.

2. Experimental

2.1. Materials

Sodium metasilicate (Na_2O_3Si), Sodium aluminate anhydrous technical grade [Al (as Al_2O_3):50-56%, Na (as Na_2O):40-45%], and sodium hydroxide anhydrous reagent grade ≥98% pellets, all purchased from Sigma Aldrich (Pty), South Africa were used for HSOD synthesis. RUB-15 was synthesized from reagent grade (98%) Tetraethyl orthosilicate (TEOS) and a 25wt.% in H_2O solution of tetramethylammonium hydroxide (TMAOH). These were procured from Sigma Aldrich (Pty), South Africa. SSOD nanoparticles were prepared by the pre-treatment of RUB-15 using propionic acid purchased from CC Imelmann Pty Ltd. The membranes were fabricated with Polysulfone (average Mw= 22 000 g/mol) beads, dissolved in N,N-dimethylacetamide ≥99.9% (Mw=87.12 g/mol) as a solvent. Synthetic AMD was prepared using $MgCl_2$, $MnCl_2.4H_2O$, Na_2SO_4, $Al(NO_3)_3$, $Fe(NO_3)_3.9H_2O$, and Ca_2OH_2 where the pH was controlled by H_2SO_4 and NaOH, all procured from Sigma Aldrich (Pty), South Africa.

2.2. Nanoparticles synthesis and fabrication of membranes

2.2.1. Nanoparticles synthesis

HSOD was synthesised by hydrothermal synthesis following a method described in the literature [6,19,22]; The precursor solution was prepared by NaOH, H_2O, Na_2SiO_3, and $NaAlO_2$ in quantities described in [6]. This solution was stirred to homogenous form then subjected to hydrothermal synthesis at 140 °C for 3.5 h in a 45 mL Teflon-lined autoclave. The sample was then centrifuged and washed severally with deionised water to a pH of 7 and allowed to dry at 100°C overnight.

A procedure described elsewhere was used to synthesize SSOD [20,21,23]. A homogenous mixture of TEOS (18.5 g) and TMAOH (32 mL) was treated in an autoclave at 140°C for seven days. The formed precipitate was rinsed with acetone. RUB-15 was then obtained by drying the particles at 60 °C for 24 h. Pre-treatment of RUB-15 was performed at a ratio of 0.1 g:30 mL of 5 M propionic acid. The pre-treated solution was agitated for 3 h and particles were recovered by centrifuge. The treated precipitate was rinsed with distilled water to a pH of 7, then dried at 60 °C for 24 hours. SSOD nanoparticles were then obtained from the calcination of the pre-treated RUB-15 particles at 600 °C for 3 h.

2.2.2. Fabrication of mixed matrix membrane

Polysulfone was dissolved in N,N-dimethylacetamide in a 10 g:50 mL ratio. Nanoparticles loading of 5 wt.% and 10wt.% were prepared and loaded into the mixture. A study by Daramola et al. [6] showed that increasing the HSOD nanoparticles loading above 10 wt.% increased the rate at which the membrane was fouled, hence, the choice of 5 wt.% and 10 wt.% nanoparticle loading in this study. Each mixture was sonicated for 10 minutes and stirred overnight. The solution was manually cast on a glass plate using “Dr. Blade”. The cast membrane was obtained by immersing in a water bath filled with deionized water (i.e., phase inversion). Impurities on membrane surface were removed by overnight soaking, after which membranes were dried at 60°C.

2.3. Characterization of nanoparticles and membranes

The morphologies of the synthesized HSOD, SSOD nanoparticles, and membranes were visualised from SEM images obtained using ZEISS scanning electron microscopy (SEM) at a voltage of 20 kV. The surface area and pore characteristics of the nanoparticles were determined by the Micrometrics Tristar 3000 (RS232) Brunauer-Emmett-Teller (BET). The nanoparticles crystallinity was analysed using Bruker XRD D2 Phaser (CuKα, λ=1.54 Å, 30 kV, and 10 mA). Scanning step size was 0.026° at a rate of 8.5°/min from 5°-90° of 2Θ. The Diffrac.Eva software was used to match the samples XRD pattern to the library. Nanoparticles functional groups were confirmed by PerkinElmer FTIR spectrometer (with deuterated triglycine sulphate (DTGS) detector and KBr beam splitter). The thermal behaviour of nanoparticles was investigated by TA instrument SDT Q600 simultaneous DSC/TGA analyser (20°C/min heating rate from 20° -800°C at 50 ml/min N_2 flow). TA.XT plus texture analyser was used for mechanical strength analysis (8.6 mm/s speed at room temperature. The sessile drop technique (OCA 15 EC GOP, Data physics) was utilized for membranes contact angle analysis with deionized water as a probe liquid dispensed at 1 µL/s. The membrane porosity (ε) was calculated using Equation 1 and membrane water uptake was determined by Equation 2.

$$\varepsilon = \frac{W_w - W_d}{\rho . V} \times 100 \quad (1)$$

$$EWC(\%) = \frac{W_w - W_d}{W_w} \times 100 \quad (2)$$

where W_w and W_d are the wet and dry weight (g) of membranes, respectively; V is the total volume of the membrane (cm^3) and ρ is the water density (0.998 $g.cm^{-3}$).

2.4. Membrane performance evaluation

A 400 mL dead-end filtration cell was used for membrane performance evaluation. Permeate flux collected after 1 h at different pressures was measured and pure water flux was calculated using Equation 3. Permeate collected was also measured to determine the membrane flux over time. Heavy metal rejections were calculated using Equation 4 where the metal cations concentrations were determined as shown in Table 1 by the Atomic Absorption Spectroscopy with the specified operating conditions and sulphate concentrations were determined by ion chromatography.

$$J_p = \frac{m_p}{At} \quad (3)$$

$$R_i = \frac{C_{fi}\text{-}C_{pi}}{C_{fi}} \times 100 \quad (4)$$

where J_p is the water flux $\left(\frac{g}{h.cm^2}\right)$, m_p is the permeate mass (g), A is the membranes effective area (32 cm^2), R_i is the metal rejection percentage, C_{fi} and C_{pi} is the of the feed and permeate concentration of metal i, respectively (mg/L) and t is the time of sample collection (h).

3. Results and Discussion

3.1. Nanoparticles characterization

SEM images of the as-produced HSOD nanoparticles show a combination of cubic shapes and thread-ball-like shapes as depicted in Fig. 1a. This confirms the formation of HSOD crystals as reported in the literature [6,25]. The presence of more than one shape could have been influenced by the synthesis time and precursor concentration [27]. The RUB-15 and SSOD nanoparticles are shown in Figs. 1b and c, respectively. A sheet-like morphology is preserved from RUB-15 to SSOD, indicating that SSOD was formed successfully without collapsing or decomposing the mother silicate layers [27]. The BET surface area of HSOD and SSOD were 201.4 and 200.5 m^2/g, respectively. The pore volume was obtained as 0.115 and 0.242 m^3/g for HSOD and SSOD, respectively. This 53% increase in pore volume indicates an improvement in the porosity of SSOD nanoparticles which can be attributed to the removal of occluded matter by topotactic conversion from the structure of the nanoparticles [21].

HSOD exhibits good crystallinity as it has sharp peaks on the XRD patterns as shown in Fig. 2a. The major peaks at 15, 25, 32, 35, and 43 2θ are consistent with pure HSOD in literature [6,17,22,26,28-30]. Fig. 2b shows the XRD pattern of SSOD and RUB-15 matched to the simulated SSOD pattern. The SSOD peaks at 12° and 21° are indicative of the successful condensation of silanol groups on adjacent layers [21]. These agree with the results reported in the literature [20,21,23,27].

Table 1
Metal concentration of synthetic AMD and AA operating parameters.

Cation	Salt	Concentration (mg/L) [24]	Sample concentration (mg/L)	Lamp current (mA)	Wavelength (nm)	Flame used (+Acetylene)
Mg^{2+}	$MgCl_2$	15	12.1	4	202.6	Air
Mn^{2+}	$MnCl_2.4H_2O$	5	31.9	5	321.7	Air
Na^{2+}	NaOH pellets	688	624.8	5	330.3	Air
Al^{3+}	$Al(NO_3)_3$	84	89.1	10	237.3	N_2O
Fe^{3+}	$Fe(NO_3)_3.9H_2O$	111	100.7	5	392	Air
Ca^{2+}	Ca_2OH_2	41	59.5	10	239.9	N_2O
SO_4^{2-}	$NaSO_4$	1108	879.7	-	-	-

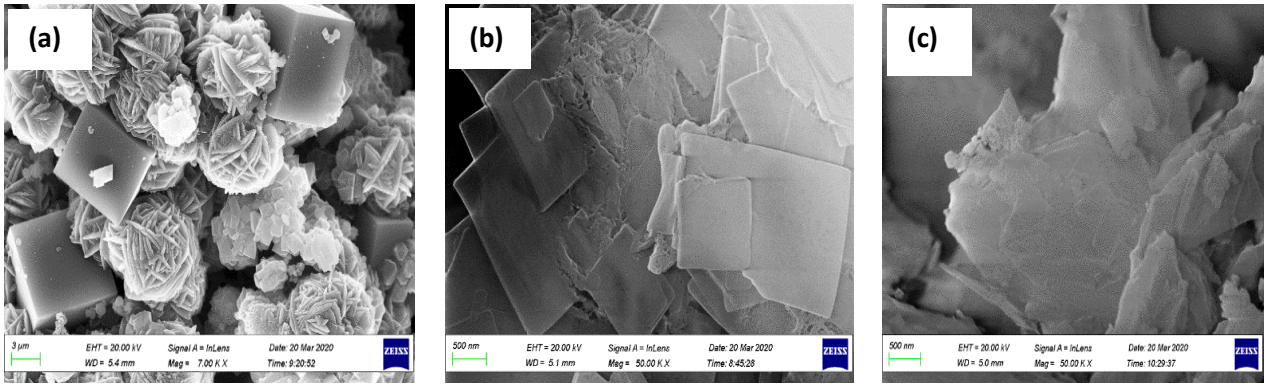

Fig. 1. SEM images of (a) HSOD (×7k), (b) RUB-15 (×50k), and (c) SSOD nanoparticles (×50k).

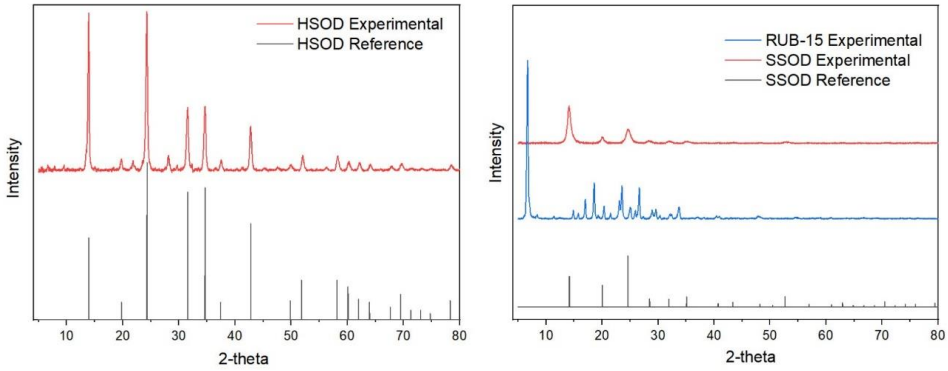

Fig. 2. XRD patterns of (a) HSOD and (b) SSOD and RUB-15.

The FTIR spectra of the nanoparticles are depicted in Fig. 3. There is an absence of CH_3 deformation vibrations at 1488 cm^{-1} and –OH bond in the 2900-3600 cm^{-1} region in the SSOD spectra when compared to the RUB-15 spectra. This indicates the removal of occluded organic matter and the absence of occluded water molecules [21]. The HSOD spectra show a sharp absorption band at ~459 cm^{-1}, indicative of the bending vibration of O-T-O (T=Si, Al) [26]. The presence of the symmetric stretch band T-O-T at 663 and 734 cm^{-1} can also be observed on the HSOD spectre [6]. The covalent bonds in the 1000-1200 cm^{-1} region (959, 1080, and 1039 cm^{-1} for HSOD, SSOD, and RUB-15, respectively) show the presence of T-O-T asymmetric stretching vibrations [31]. According to AlOweini et al. [31], the stretching vibration band centred at ~ 959 cm^{-1} for HSOD is also indicative of the silanol (SiOH) group. Similar FTIR spectra were obtained in literature [21,26,31].

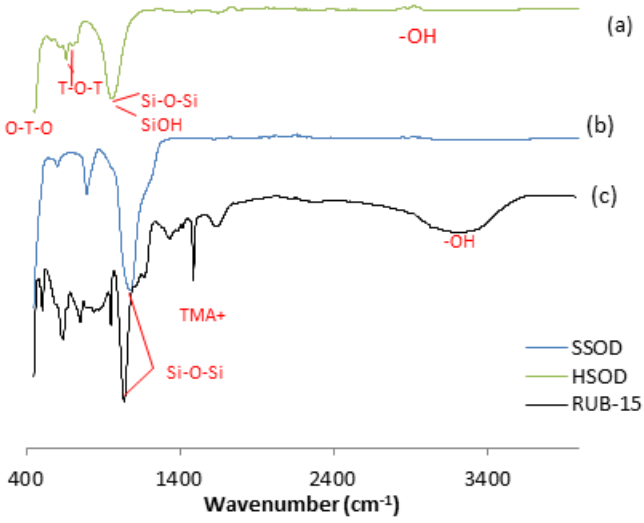

Fig. 3. FTIR spectra of (a) HSOD, (b) SSOD and (c) RUB-15.

The thermal behaviour of the nanoparticles is illustrated in Fig. 4. The weight loss below temperatures of 140 °C is associated with the loss of physically absorbed water. At temperatures above 140 °C, there is a gradual weight loss (1.4 %) for SSOD, indicating the removal of propionic acid in the SSOD nanoparticles [27]. Weight loss above 350 °C for HSOD indicates the decomposition of all water molecules in the cell structure, resulting in structural collapse [22]. These correspond to results reported in the literature [22,27].

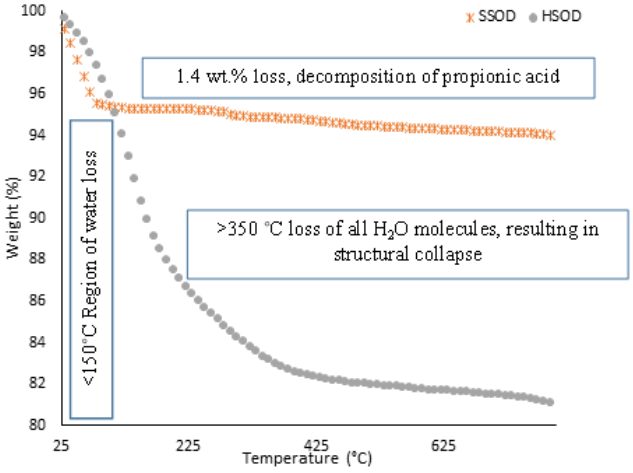

Fig. 4. TG analysis of SSOD and HSOD nanoparticles.

3.2. Characterization of fabricated mixed matrix membranes

Fig. 5 depicts the SEM cross-sectional images of (a) PSf, (b) 5%HSOD/PSf, (c) 5%SSOD/PSf, (d) 10%HSOD/PSf, and (e) 10%SSOD/PSf. The cross-section of the PSf membrane in Fig. 5a shows a porous structure with a dense skin layer. The nanoparticles-loaded membranes (Fig. 5b-e) show the successful infusion of the nanoparticles into the polymer membrane. It is worth noting that there is an uneven distribution of nanoparticles in the membranes. This could be attributed to the agglomeration of the particles within the fractional free volume of the polymer due to the poor dispersion as reported by Daramola et al. [6].

Membranes show an improvement in water affinity when loaded with HSOD as shown by the reduced contact angle and increased porosity in Fig. 6. The 10%HSOD/PSf and 5%HSOD/PSf membranes had the lowest contact angle of 79° and 78°, respectively. They also had the highest porosity of 40% and 18%, respectively. This can be attributed to the hydrophilic HSOD nanoparticles. Comparable outcomes were achieved in the literature [32]. The infusion of 10%SSOD nanoparticles into PSf had no impact on the contact angle of the membrane. However, the presence of the SSOD nanoparticles reduced the porosity of the membranes from 16% for PSf to 9.6% and 3.8% for 10%SSOD/PSf and 5%SSOD/PSf, respectively. The membrane porosity was calculated by the relationship between the wet and dry membrane given by Equation 1. The reduction of porosity in the presence of SSOD nanoparticles can be attributed to the poor absorption of water by the membrane because of the presence of the hydrophobic nanoparticles. This phenomenon can be better explained by the principle of membrane wettability. Yao et al. [33] define membrane wettability as the contact of a liquid with a membrane surface through intermolecular interactions between the surface, liquid, and gas. The liquid penetrates the pores of the membrane resulting in pore obstruction. This is more pronounced in membranes with small contact angles [33].

The mechanical strength of the membranes is shown in Fig. 7. The results showed a reduction in the Young modulus for the 10% HSOD/PSf membrane when compared to that of the 5%HSOD/PSf membrane. This can be an indication of particle agglomeration at higher loadings [6]. On the contrary, infusing the SSOD nanoparticles resulted in an 18 % increase of the Young Modulus whereas the tensile strength was reduced by 9 % when compared to that of the PSf membrane. A similar trend was observed by Eden et al. [21], and this was attributed to the interaction between the polymer and nanoparticle agglomerates that further restricts the polymer chain movement.

3.3. Membrane performance evaluation

3.3.1. Effect of pressure on pure water flux

Membranes' pure water flux was evaluated at varying pressures as shown in Fig. 8. An increase in flux at increasing pressures can be observed. Similar results were obtained in the literature [34,35]. This is because of the increased driving force which improves mass transfer [36,37]. The enhanced flux of HSOD loaded membranes when compared to the PSf membrane is due to the improved permeation channels created by the HSOD nanoparticles with a cage diameter of ~2.6 Å which allow the water molecules (kinetic diameter ~2.65Å) to pass easily [6]. It can be observed that the membranes loaded with SSOD have the highest flux in all evaluated transmembrane pressures. According to Vatanpour, et al. [34], the membrane's hydrophilicity, pore size, and structure influence its permeability. The highest contact angle (88.4 °C) and low porosity (9.6 %) were observed in the 10%SSOD/PSf membrane, indicating that it is hydrophobic. The membrane's porosity was defined in terms of the membrane's ability to absorb water (Equation 1). The SSOD membranes showed that they could not retain water, but because of the higher SSOD nanoparticles pore volume obtained from BET, they do allow more water to pass through them. Enhanced permeability can be attributed to the SSOD pore volume obtained from BET (0.242 m^3/g) which is 53 % more than that of HSOD, hence the improved flux. Similar results were obtained by Fernandes et al. [38] by comparing polyvinylidene difluoride (PVDF) membranes infused with hydrophobic and hydrophilic silica. The membranes loaded with hydrophobic silica showed a high contact angle, however, the membrane water flux was higher than when compared to the membrane infused with hydrophilic silica.

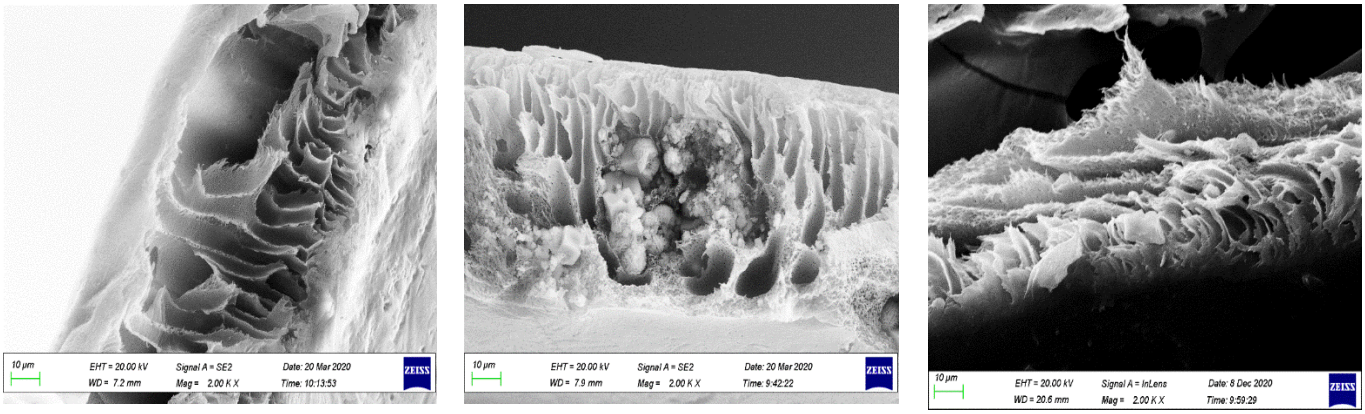

Fig. 5. Cross sectional SEM images of (a) PSf (×2k), (b) 5%HSOD/PSf (×2k), (c) 5%SSOD/PSf (×2k), (d) 10%HSOD/PSf (×2k), and (e) 10%SSOD/PSf (×2k).

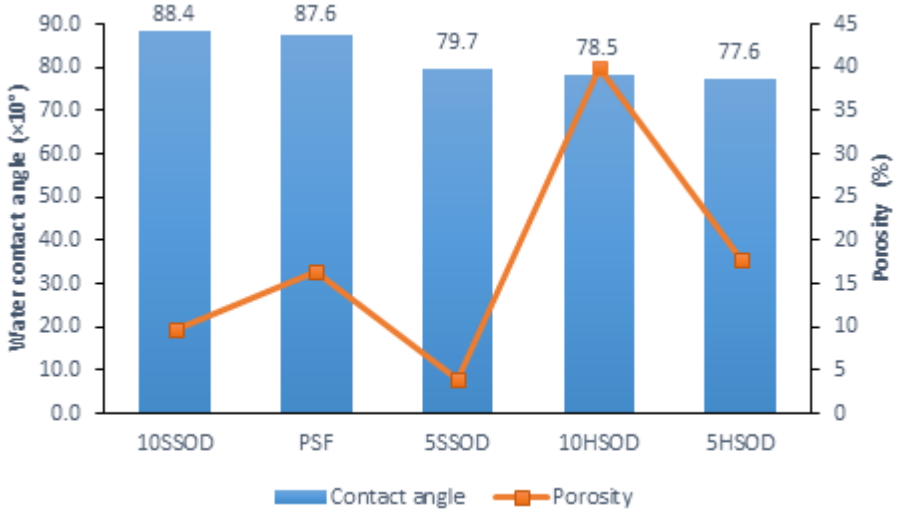

Fig. 6. Membranes contact angle and porosity.

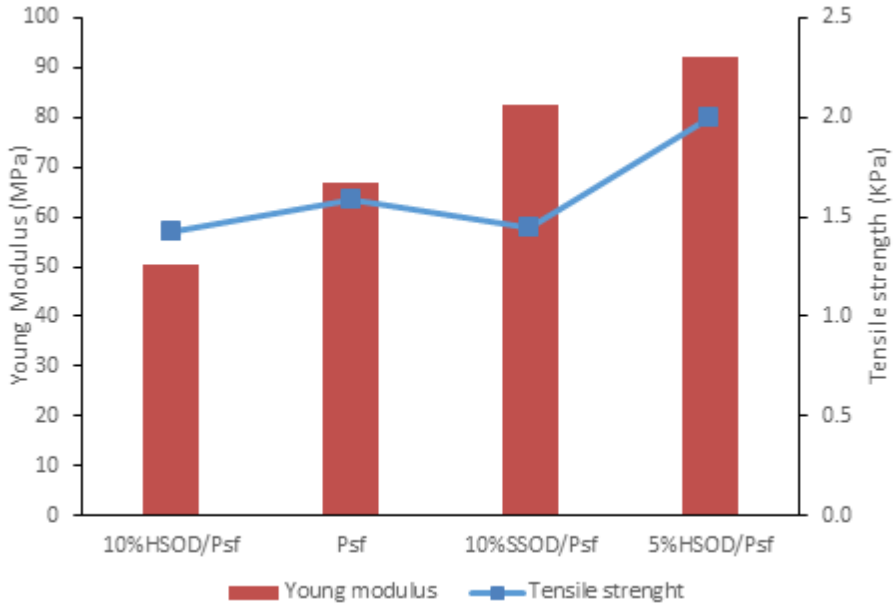

Fig. 7. Mechanical strength of the fabricated membranes.

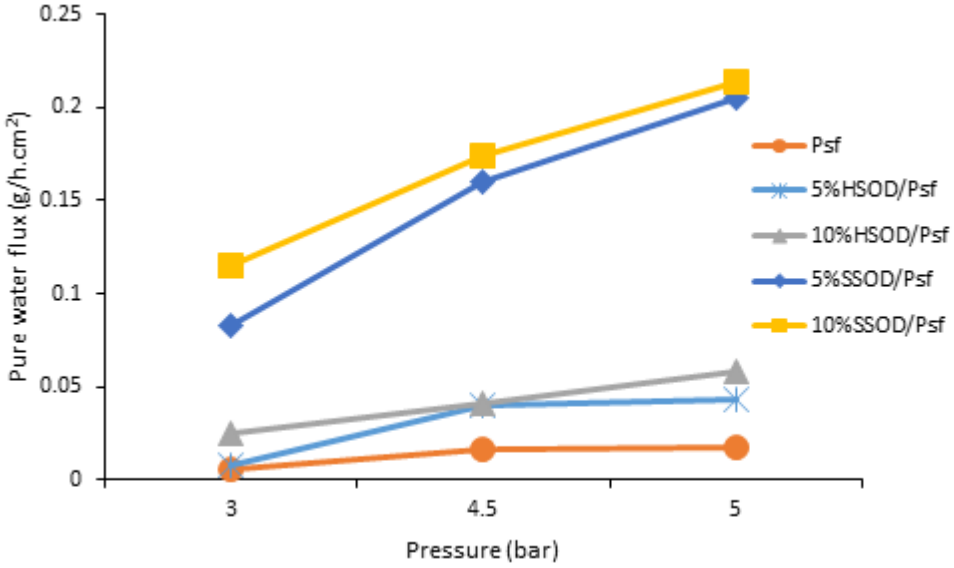

Fig. 8. Membranes pure water flux.

3.3.2. Effect of nanoparticles loading on membrane flux

The membranes solution flux collected over operation time is presented in Fig. 9. A decline in flux over the evaluated period is a general trend for all the membranes. This is because of the accumulation of the retentate particles over time which obstructs the pore channels of the membranes, hence reducing the flow of water. This phenomenon is described in the literature in one of four mechanisms of fouling (complete blocking of pores, intermediate blocking of pores, constriction of pores, and cake layer formation) [39,40]. The infusion of nanoparticles into PSf reduced the fouling rate as PSf had a 93 % reduction in flux. Presence of nanoparticles in the fabricated membranes resulted in percentage flux reduction of 77 %, 65 %, 58 % and 54 %, for 5%HSOD/PSf, 5%SSOD/PSf, 10%SSOD/PSf, and 10%HSOD/PSf, respectively. This is because the foulants are more likely to accumulate on the surface of the hydrophobic PSf [41,42]. Although 10%SSOD/PSf showed a high contact angle than PSf indicating that it is more hydrophobic. The low fouling rate on SSOD loaded membranes when compared to PSf can be explained by the high flux of SSOD loaded membranes as presented in Fig. 8. At the investigated time, the SSOD membranes were able to maintain a higher flux over time, though foulants were mounting on the surface of the membrane. Because of the relatively low rate of deposition of the foulants in comparison to the high permeability of the membranes, a reduction in the membrane flux was barely noticeable. This implies that the infusion of nanoparticles into the polymer reduced the fouling rate of the membrane. These results are consistent with the literature [41,42].

3.3.3. Effect of nanoparticles loading on metal rejection

The effect of nanoparticle loadings on the heavy metals rejection from the different membranes is depicted in Fig. 10. Maximum rejections of 89.1 %, 74.7 %, 65.8 %, 61.5 %, 57.4 % and 37.7 % were obtained for Al^{3+}, Mg^{2+}, Fe^{3+}, Mn^{2+}, Ca^{2+}, and Na^{2+}, respectively as shown in Fig. 10. The 10%HSOD/PSf membrane shows the capability of rejecting all the evaluated metal ions, whereas other membranes are only able to reject a few ions. This can be

attributed to the HSOD small pore diameter as smaller particles sizes are favourable because they can provide a more polymer/particle interfacial area, hence improved separation [43,44]. The 5%SSOD/PSf membrane showed a promising metal rejection as it is second to the 10%HSOD/PSf in rejection. The SSOD loaded membranes were able to produce high flux at 10wt.% loading and improved rejections at 5wt.% loading. The poor rejection can be attributed to particles agglomeration at higher loadings resulting in pore blocking, hence an increase in mass transfer resistance [21]. This can be overcome by the functionalization of nanoparticles to create an even distribution of nanoparticles [6].

4. Conclusions

SSOD and HSOD nanoparticles were synthesized successfully via topotactic conversion and hydrothermal synthesis, respectively. Successful infusion of these nanoparticles was confirmed by SEM images which showed nanoparticles agglomeration at increased loadings. The highest pure water flux obtained was 0.21 $g.h^{-1}.cm^{-2}$ for 10%SSOD/PSf at 5 bar. Highest selectivity was obtained from the 10%HSOD/PSf membrane with rejections of 75%, 66%, 61%, 57%, 52%, and 38% for Mg^{2+}, Fe^{3+}, Mn^{2+}, Ca^{2+}, $Al^{3+}$and Na^{2+}, respectively. However, this membrane showed one of the least pure water fluxes (0.06 $g.h^{-1}.cm^{-2}$). The reduced flux resulted in good metal rejections, indicating the trade-off between selectivity and permeability. These results show that both HSOD and SSOD have potential for AMD treatment. Although HSOD loaded membranes showed good selectivity, there is little that can be done to improve the permeability as HSOD pores are occluded with water molecules, and removing them will result in structural collapse. On the other hand, the poor selectivity of SSOD loaded membranes can be improved by improving the dispersion of nanoparticles. The results obtained in this study could be a platform to improve the SSOD infused membranes for heavy metal removal.

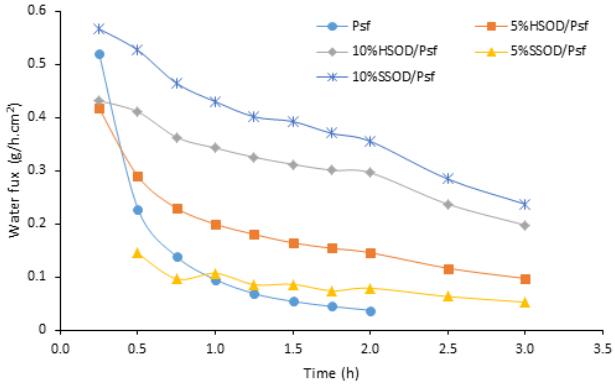

Fig. 9. Membrane flux over time.

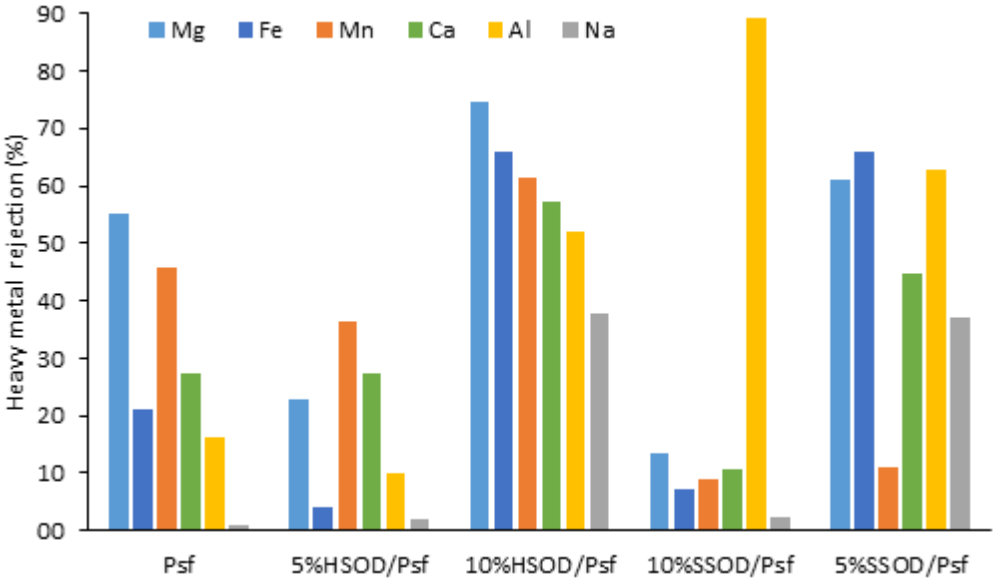

Fig. 10. Heavy metal rejection.

Author's contribution

The manuscript was written through equal contributions of N.C.N, O.O.S., and M.O.D. N.C.N, O.O.S., and M.O.D. have approved the final version of the manuscript.

Funding

This research was funded by the University of the Witwatersrand.

Acknowledgments

The authors are grateful to the Sustainable Energy and Environment Research Unit (SEERU) members, the Microscopy and Microanalysis Unit (MMU) staff of the University of the Witwatersrand, for assisting with the equipment, the School of Chemical and Metallurgical engineering staff of the University of the Witwatersrand, for the technical support and the financial support provided by CSIR.

Conflicts of interest

The authors declare no conflicts of interest.

References

[1] Choudhury, B. U., Malang, A., Webster, R., Mohapatra, K. P., Verma, B. C., Kumar, M., Hazarika, S., Acid Drainage from Coal Mining: Effect on Paddy Soil and Productivity of Rice. Sci. Total. Environ., (2017) 344-351. doi:10.1016/j.scitotenv.2017.01.074

[2] Aguiar, A. O., Andrade, L. H., Ricci, B. C., Pires, W. L., Miranda, G. A., & Amaral, M. C., Gold Acid mine Drainage Treatment by Membrane Separation Process: An Evaluation of the Main Operational Conditions. Sep. Purif. Technol., (2016) 360-369. Doi:10.1016/j.seppur.2016.07.003

[3] Moodley, I., Sheridan, C. M., Kappelmeyer, U., & Akcil, A., . Environmentally Sustainable Acid Mine Drainage Remediation: Research Developments with a Focus on Waste/By-Products. Miner. Eng., (2018) 207-220. Doi:10.1016/j.mineng.2017.08.008

[4] Taylor, J., Pape, S., & Murphy, N., A Summary of Passive and Active Treatment Technologies for Acid and Metalliferous Drainage (AMD). Fifth Australian Workshop on Acid Drainage. Frematle, Western Australia: Earth Systems Pty Ltd, 2005.

[5] Kefeni, K. K., Msagati, T. A., & Mamba, B. B., Acid Mine Drainage: Prevention, Treatment Options, and Resource Recovery: A review. J. Clean. Product., (2017) 475-493. doi:10.1016/j.jclepro.2017.03.082

[6] Daramola, M. O., Silinda, B., Masondo, S., & Oluwasina, O. O., Polyethersulfone-Sodalite (PES-SOD) Mixed-Matrix Membranes: Prospects for Acid Mine Drainage (AMD) Treatment. J. S. Afr. Inst. Min. Metall., (2015) 1221-1228. doi:10.17159/2411-9717/2015/v115n12a11

[7] Lopez, J., Reig, M., Gibert, O., Valderrama, C., & Cortina, J., Evaluation of NF Membranes as Treatment Technology of Acid Mine Drainage: Metals and Sulfate Removal. Desal., (2018) 440, 122-134. doi: 10.1016/j.desal.2018.03.030

[8] Mathaba, M., & Daramola, M. O., Effect of Chitosan's Degree of Deacetylation on the Performance of PES Membrane Infused with Chitosan during AMD Treatment. Membr.. (2020) doi:10.3390/membranes10030052

[9] Hull, E., & Zodrow, K., Acid Rock Drainage Treatment Using Membrane Distillation: Impacts of Chemical-Free Pre-treatment on Scale Formation, Pore Wetting, and Product Water Quality. Environ. Sci. Technol., 51 (2017) 11928-11934. doi: 10.1021/acs.est.7b02957

[10] Direct Contact Membrane Distillation. [PDF]. Retrieved 20 January 2022, from https://www.lenntech.com/Data-sheets/MD-ZLD-interactive.pdf, (n.d)

[11] Masindi, V., Osman, M., & Abu-Mahfouz, A., Integrated Treatment of Acid Mine Drainage using BOF Slag, Lime/Soda Ash, and Reverse Osmosis (RO): Implication for the Production of Drinking Water. Desal., (2017) 424, 45-52. doi: 10.1016/j.desal.2017.10.002

[12] Squires, R., Removal of Heavy Metals from Industrial Effluent by Crossflow Microfiltration. Water. Sci. Technol., 25(10), (1992) 55-67. doi: 10.2166/wst.1992.0237

[13] Pandya, J., Nanofiltration for Recovery of Heavy Metal from Waste Water. MSc Report. (2015) doi: 10.13140/RG.2.1.5040.7524

[14] Barakat, M., & Schmidt, E., Polymer-Enhanced Ultrafiltration Process for Heavy Metals Removal from Industrial Wastewater. Desal., 256 (2010) 90-93. doi: 10.1016/j.desal.2010.02.008

[15] Tetala, K. K., & Stamatialis, D. F., Mixed Matrix Membranes for Efficient Adsorption of Copper Ions from Aqueous Solutions. Sep. and Purif. Technol., (2013) 214–220. doi:10.1016/j.seppur.2012.11.022

[16] Habiba, U., Afifi, A. M., Salleh, A., & Ang, B. C., Chitosan/(Polyvinyl Alcohol)/Zeolite Electrospun Composite Nanofibrous Membrane for Adsorption of Cr6+, Fe3+, and Ni2+. J. Hazard. Mater., (2017) 182-194. doi: 10.1016/j.jhazmat.2016.06.028

[17] Golbad, S., Khoshnoud, P., & Abu-Zahra, N., Hydrothermal Synthesis of Hydroxy Sodalite from Fly Ash for the Removal of Lead Ions from Water. Int. J. Environ. Sci. Technol., 14 (2016) 135-142. doi: 10.1007/s13762-016-1133-x

[18] Khajavi, S., Jansen, J. C., & Kapteijn, F., Application of Hydroxy Sodalite Films as Novel Water Selective Membranes. J. Membr. Sci., (2009) 153–160. doi:10.1016/j.memsci.2008.09.046

[19] Khajavi, S., Jansen, J. C., & Kapteijn, F., Production of Ultrapure Water by Desalination of Seawater using Hydroxy Sodalite Membrane. J. Membr. Sci., (2010) 52-57. Doi:10.1016/j.memsci.2010.03.026

[20] Moteki, T., Chaikittisilp, W., Shimojima, A., & Okubo, T., Silica Sodalite without Occluded Organic Matters by Topotactic Conversion of Lamellar Precursor. Am. Chem. Soc., (2009) 15780–15781. doi: 10.1021/ja806930h

[21] Eden, C. L., & Daramola, M. O., Evaluation of Silica Sodalite Infused Polysulfone Mixed Matrix membranes during H2/CO2 Separation. Mater. Today, (2020) doi: 10.1016/j.matpr.2020.02.393

[22] Khajavi, S., Sartipi, S., Gascon, J., Jansen, J. C., & Kapteijn, F., Thermostability of Hydroxy Sodalite in view of Membrane Applications. Microporous and Mesoporous Mater., (2010) 510-517. doi:10.1016/j.micromeso.2010.03.035

[23] Koike, M., Asakura, Y., Sugihara, M., Kuroda, Y., Tsuzura, H., Wada, H., & Kuronda, K., Topotactic Conversion of Layered Silicate RUB-15 to Silica Sodalite through Interlayer Condensation in N-methylformamide. R. Soc. Chem., (2017) 10232–10239. doi:10.1039/c7dt01287j

[24] Bell, F. G., Bullock, S. E., Halbich, T. F., & Lindsay, P., Environmental Impacts Associated with an Abandoned Mine in the Witbank Coalfield, South Africa. Int. J. Coal Geol., (2001) 195–216. doi: 10.1016/S0166-5162(00)00033-1

[25] Kundu, D., Dey, B., Naskar, M. K., & Chatterjee, M., Emulsion-Derived Urchin-Shaped Hydroxy Sodalite Particles. Mater. Lett., (2010) 1630-1633. doi:10.1016/j.matlet.2010.04.015

[26] Naskar, M. K., Kundu, D., & Chatterjee, M., Effect of Process Parameters on Surfactant Based Synthesis of Hydroxy Sodalite. Mater. Lett., (2011) 463-438. doi:10.1016/j.matlet.2010.11.008

[27] Moteki, T., Chaikittsilp, W., Sakamoto, Y., Shimojima, A., & Okubo, T., Role of Acidic Pre-treatment of Layered Silicate RUB-15 in its Topotactic Conversion into Pure Silica Sodalite. Chem. Mater., (2011) 3564–3570. doi:10.1021/cm201480x

[28] Musyoka, N. M., Petrik, L. F., Balfour, G., Gitari, W. M., & Hums, E., Synthesis of Hydroxy Sodalite from Coal Fly Ash Using Waste Industrial Brine Solution. J. Environ. Sci. Health, Part A, (2011) 1699–1707. doi:10.1080/10934529.2011.623961

[29] Nabavi, M. S., Mohammadi, T., & Kazemimoghadam, M., Hydrothermal Synthesis of Hydroxy Sodalite Zeolite Membrane: Separation of H2/CH4. Ceram. Int.l, (2014) 5889–5896. doi:10.1016/j.ceramint.2013.11.033

[30] Eterigho-Ikelegbe, O., Bada, S., Daramola, M. O., & Falcon, R., Synthesis of High Purity Hydroxy Sodalite Nanoparticles via Pore-Plugging Hydrothermal Method for Inorganic Membrane Development: Effect of Synthesis Variables on Crystallinity, Crystal Size, and Morphology. Mater. Today: Proc, (2020) doi:10.1016/jmatpr.2020.03.639

[31] Al-Oweini, R., & El-Rassy, H., Synthesis and Characterization by FTIR Spectroscopy of Silica Aerogels Prepared Using Several Si(OR)4 and R" Si(OR')3 Precursors. J. Mol. Struct., 140145 (2009) doi:10.1016/j.molstruc.2008.08.025

[32] Ngobeni, R., Sadare, O., & Daramola, M., Synthesis and Evaluation of HSOD/PSF and SSOD/PSF Membranes for Removal of Phenol from Industrial Wastewater. Polym., 13 (2021) 1253. doi: 10.3390/polym13081253

[33] Yao, M., Tijing, L., Naidu, G., Kim, S., Matsuyama, H., Fane, A., & Shon, H., A Review of Membrane Wettability for the Treatment of Saline Water Deploying Membrane Distillation. Desal., 479 (2020) 114312. doi: 10.1016/j.desal.2020.114312

[34] Vatanpour, V., Madaeni, S. S., Moradian, R., Zinadini, S., & Astinchap, B., Fabrication and Characterization of Novel Antifouling Nanofiltration Membrane Prepared from Oxide Multiwalled Carbon Nanotube/ Polyethersulfone Nanocomposite. J. Membr. Sci., (2011) 284-294. doi:10.1016/j.memsci.2011.03.055

[35] Zhong, C.-M., Xu, Z.-L., Fang, X.-H., & Cheng, L. (2007). Treatment of Acid Mine Drainage (AMD) by Ultra-Low-Pressure Reverse Osmosis and Nanofiltration. Environ. Eng. Sci., (2007) 1297-1306. doi:10.1089/ees.2006.0245

[36] Rameetse, M. S., Aberefa, O. A., & Daramola, M. O. (2019). Synthesis and Characterization of PSF/PES Composite Membranes for Use in Oily Wastewater Treatment. J. Phys.: Conf. Ser., (2019) 1378. doi:10.1088/1742-6596/1378/2/022013

[37] Sadare, O., & Daramola, M., Blended Polysulfone/Polyethersulfone (PSF/PES) Membrane with Enhanced Antifouling Property for Separation of Succinate from Organic Acids from Fermentation Broth. ACS Sustain. Chem. Eng., 9 (2021) 13068-13083. doi: 10.1021/acssuschemeng.1c05059

[38] Fernandes, C., Md Nordin, N., Bilad, M., Matsuura, T., Putra, Z., Wirzal, M., & Jaafar, J. (2021). Explication of Hydrophobic Silica as Effective Pore Former for Membrane Fabrication. Appl. Surf. Sci. Adv., 3 (2021) 100051. doi: 10.1016/j.apsadv.2020.100051

[39] Aly, S., Ph.D. Thesis: Pre-Treatment Evaluation Prior to Ultrafiltration in Secondary Effluent Treatment for Water Reuse. Waterloo: University of Waterloo, 2005

[40] Abbasi, M., Sebzari, M. R., Salahi, A., & Mirza, B., Modelling of Membrane Fouling and Flux Decline in Microfiltration of Oily Wastewater using Ceramic Membranes. Chem. Eng. Commun., (2012) 78-93. doi:10.1080/00986445.2011.570391

[41] Ahmad, A. L., Majid, M. A., & Ooi, B. S., Functionalized PSf/SiO2 Nanocomposite Membrane for Oil-in-Water Emulsion Separation. Desal., (2011) 266-269. doi:10.1016/j.desal.2010.10.017

[42] Kumar, R., & Ismail, A. F., Fouling Control on Microfiltration/Ultrafiltration Membranes: Effects of Morphology, Hydrophilicity. J. Appl. Polym. Sci., (2015) 42042-42053. doi: 10.1002/app.42042

[43] Bose, S., & Mahanwar, P. A., Effect of Particle Size of Filler on Properties of Nylon-6. J. Miner. Mater. Charact. Eng., (2004) 23-31. doi:10.4236/jmmce.2004.31003

[44] Chung, T.-S., Jiang, L. Y., & Kulprathipanja, S., Mixed Matrix Membranes (MMMs) Comprising Organic Polymers with Dispersed Inorganic Fillers for Gas Separation. Prog. Polym. Sci., (2007) 483-507. doi:10.1016/j.progpolymsci.2007.01.008